UNSTEADY THERMAL CONVECTION OF MELTS IN A 2-D HORIZONTAL BOAT IN A CENTRIFUGAL FIELD WITH CONSIDERATION OF THE CORIOLIS EFFECT

F. Tao,[1] Y. Zheng,[1] W.J. Ma[1] and M.L. Xue[1]

[1] Institute of Mechanics
Chinese Academy of Sciences
Beijing 100080, China

ABSTRACT

A rotating centrifuge introduces the centrifugal acceleration and the Coriolis force acting on melts while melt growth is being carried out in the centrifuge. These two forces influence melt convection and, in turn, modify the transport of dopant and impurities. In this paper the effects of varying the centrifugal acceleration and the Coriolis force were studied numerically. We paid attention to unsteady thermal convection of melts in a two-dimensional rectangular boat with relevance to crystal growth in a centrifuge by horizontal Bridgman technique. The mathematical model was constructed by the continuity, Navier-Stokes and energy equations with the Boussinesq approximation, which was solved by the finite control volume method with fully implicit, steady, time-marching, central-difference discretization. The calculations based on the simplified model reveal that the centrifugal acceleration enhances buoyancy force, which may dominate the convection and induce oscillation, and the Coriolis force may stabilize or destabilize the flow depending on the rotation sense of the centrifuge. This numerical results as well as the experiments of temperature measurement[15] give a satisfactory explanation of the results described previously[12,13].

INTRODUCTION

In crystal growth from melts, convection in the melt is of great importance in determining the quality and compositional uniformity of the grown crystal because it is usually oscillatory or fluctuating flow that causes compositional striations in the crystal. In order to grow single crystal within the environment of a stabilized melt crystal grower has to treat the growth system carefully. However, one only with experience obviously can not satisfy the increasing demand for more perfect single crystals (e.g. Si and GaAs). Thus,

Materials Processing in High Gravity, Edited by L.L. Regel
and W.R. Wilcox, Plenum Press, New York, 1994

scientists, such as Carruthers[1], Langlois[2] and Müller[3], exerted themselves much to study the role of melt convection and the relevant mechanisms in crystal growth.

Gravitational effect is in general important, and even dominant, to thermal convection of melts unless melt growth is carried out in microgravity environment. It has been well known that growth of crystals in such environment has more advantages than on earth because microgravity effect hinders buoyancy convection. Unexpectedly, in recent years, when Müller and his colleagues studied the gravitational effect on crystal growth, they found that single crystal also could be grown under high gravity, i.e. the centrifugal acceleration produced by a centrifuge.[3-9] Using the centrifuge in their laboratory, they grew InSb and GaSb crystals free of doping striations by an upside-down, tilted Bridgman method and a horizontal zone melting technique. Their finding now fascinates many crystal growers and scientists who have begun to do research work on this interesting subject.[10-15]

From the initial purpose of their experimental research it is natural for Müller et al. to attribute the results to the effect of high gravity. However, it must be noted that a centrifugal field does not produce high gravity monotonically. Besides the centrifugal acceleration, the Coriolis force simultaneously occurs in the melt and alters convection in the same centrifugal field. Certainly, when these two forces act in concert the flow structures are not in a simple form but quite complex. Thus, a more careful investigation on this problem is still needed. After a series of research work through experiments and numerical simulations, Müller et al. observed that steady convection could occur in the melt, and concluded in their review paper[9] that the steady phenomena were not due to high gravity but the effect of the Coriolis force. For a different arrangement Regel et al. presented a dissimilar opinion on the subject.[10,11,14]

Unlike the methods used by Müller et al. and Regel et al., we take special interest in the horizontal Bridgman technique. Results of the GaAs crystals grown in a large centrifuge showed that the impurity striations became weak or less dense than their original ones[12,13]. In order to obtain more understanding of convection under high gravity we carried out a model experiment of temperature measurement with molten Sn in the same centrifuge.[15] Interesting phenomena due to the Coriolis effect were also observed in this model experiment.

However, up to now we have only limited experimental data, which led to an incomplete understanding of the behavior of the melt in the horizontal Bridgman technique in the centrifuge. To understand and explain the melt behavior comprehensively, we need more information on the flow field. For the horizontal Bridgman technique, there is a problem of finding a method for direct observation of the melt flow, not to mention the difficulties in performing experiments in the centrifuge. Thus, we carried out a numerical simulation to serve these requirements.

In this research the effects of varying the centrifugal acceleration and the Coriolis force were studied numerically. We paid attention to time-dependent thermal convection of melts in a two-dimensional, rectangular configuration of open boat with relevance to crystal growth in a centrifuge by horizontal Bridgman technique. In section 2 we describe the physical problem and discuss construction of the numerical model. Next, in section 3 we introduce time-dependent continuity, Navier-Stokes (with Boussinesq approximation) and energy equations in primitive variables. After section 3 we present the grid system and the algorithm for the calculation. Section 5 gives the numerical results. Finally, we draw some conclusions on the phenomena of convective flow in horizontal Bridgman technique in a centrifugal field.

DESCRIPTION OF THE PHYSICAL MODEL

The experimental arrangement of horizontal gradient freeze method in the large

centrifuge described previously[12,13] is schematically pictured in Figure 1. An open boat in the shape of a semi-circular horizontal cylinder was positioned within a horizontal furnace and subjected to a temperature gradient. To prevent the melt from spilling out of the boat during experiments the furnace, mounted at the end of the arm of the centrifuge, was hinged on the beam so that it would align itself with the resultant gravity vector **g**. Therefore, the upper surface of the melt was flat and stationary with respect to **g**.

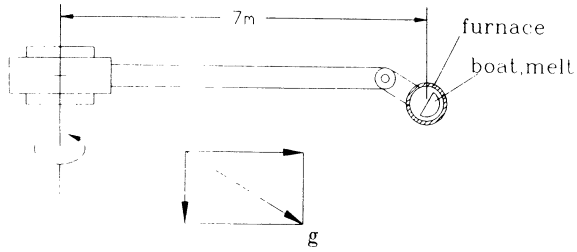

Figure 1. Sketch of crystal growth by the horizontal Bridgman technique in the large centrifuge.

For melt convection in a horizontal boat, a two-dimensional simulation is usually considered necessary to show some of the main characteristics of the real flow structure. However, at present, it is difficult for us to carry out this calculation because the buoyancy effects of both earth gravity and centrifugal acceleration, along with the Coriolis effect, may result in three-dimensional convection.

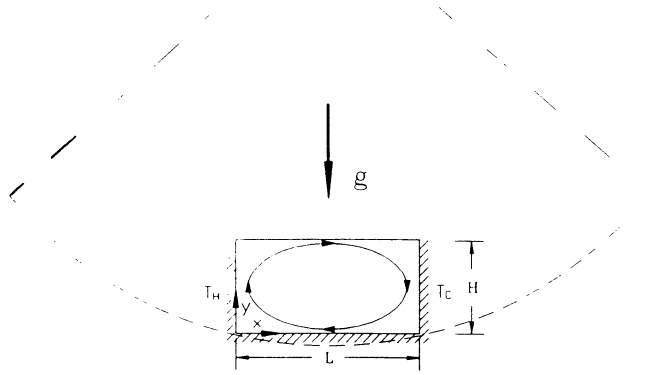

Figure 2. Configuration of the two-dimensional horizontal rectangular boat for the simulation of melt flow in a centrifugal field.

We now set some assumptions for the two-dimensional model. First we eliminate earth gravity and assume that the buoyancy effect on melt convection is solely caused by centrifugal acceleration. If, for example, the centrifugal acceleration is six times earth gravity, the furnace will lie on a position near the plane of the arm of the centrifuge with the angle less than 10°. In this case, the buoyancy should be regarded as dominated by the centrifugal acceleration. Under the above assumption, the influence of earth gravity

therefore could be neglected and the centrifugal acceleration would be perpendicular to the melt surface. This two-dimensional idealized model is shown in Figure 2. It has a rectangular configuration of length L and thickness H. The upper boundary is the free surface of the melt. Both vertical side-walls are assumed to be held at different temperatures, T_H at the left and T_C at the right, respectively, with $T_H > T_C$. Here, we do not consider the case where T_C is lower than the melting-point T_m, but rather $T_C > T_m$. Then, standing on the centrifuge one would observe that the melt moves in a clockwise sense for either direction of centrifuge rotation.

The Coriolis force entailed in a centrifugal field as well as the buoyancy effect of the centrifugal acceleration has also a vital influence on the convection. Indeed, if the Coriolis force did not occur in the centrifugal field the simulation could be treated as those described by Crochet et al.[16] and Fontaine et al.[17] for conventional growth. Analysis shows that its effect cannot be ignored. From the definition of the Coriolis force, $\boldsymbol{f}_c = -2\boldsymbol{\omega} \times \mathbf{u}$, two different effects of the Coriolis force can act on melt flow. For example, if only one single convective cell occurs in the boat as in Figure 2, these effects, I and II, will take place as shown in Figure 3. They depend strongly on the rotation sense of the centrifuge, similar to that described by Müller et al.[9]. We discuss the results related to this problem in section 5.

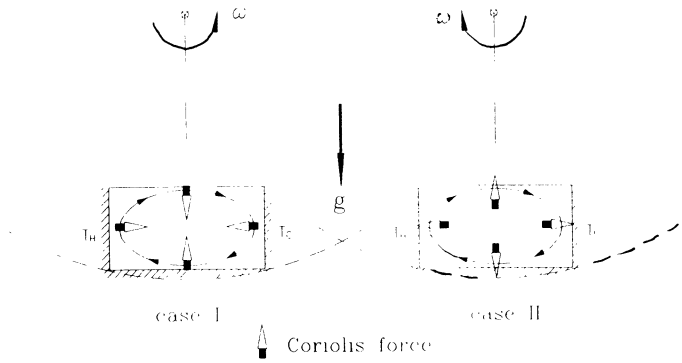

Figure 3. The two patterns of the Coriolis effect on melt convection in the horizontal Bridgman boat, depending on the direction of rotation of the centrifuge.

GOVERNING EQUATIONS AND BOUNDARY CONDITIONS

Let us consider the simplified model in Figure 2. The boat and the two-dimensional coordinate system are both fixed on the arm of the centrifuge, and turn around the axis of the centrifuge when the centrifuge operates. The fundamental flow field variables are the two velocity components u and v, pressure p, and temperature T. The governing equations are:

$$\nabla \cdot \mathbf{u} = 0, \tag{1}$$

$$\frac{\partial \mathbf{u}}{\partial t} + (\mathbf{u} \cdot \nabla)\mathbf{u} = -\frac{1}{\rho}\nabla p + \nu \nabla^2 \mathbf{u} + \beta \mathbf{g}(T - T_C) - 2\boldsymbol{\omega} \times \mathbf{u}, \tag{2}$$

$$\frac{\partial T}{\partial t} + (\mathbf{u} \cdot \nabla)T = \kappa \nabla^2 T, \tag{3}$$

where $\mathbf{u}$ denotes the velocity vector of the flow field, $\boldsymbol{\omega}$ the angular velocity vector of the

centrifuge, ρ the density of the melt, ν the kinematic viscosity, β the volumetic expansion coefficient and κ the thermal diffusivity. Equations 1-3 are the continuity equation, Navier-Stokes equation, and energy equation, respectively. In equation 2 the validity of the Boussinesq approximation is presumed. The term $-2\boldsymbol{\omega}\times\mathbf{u}$ is the Coriolis force.

In order to obtain a general understanding of melt behavior, we perform the simulation in a dimensionless form. However, it must be noted that there is no obviously typical velocity scale for us to select. Necessarily it should be obtained from momentum balance. Since the buoyancy force dominates convection in the present problem, the magnitudes of terms $(\mathbf{u}\cdot\nabla)\mathbf{u}$ and $\beta\mathbf{g}(T-T_C)$ in equation 2 should be considered the same. Then we have:

$$(\mathbf{u}\cdot\nabla)\mathbf{u}\sim\beta\mathbf{g}(T-T_C), \tag{4}$$

or in terms of typical parameters equation 4 become:

$$\frac{UH}{\nu}=O(Gr^{1/2}), \tag{5}$$

where H is the typical length scale, U the typical velocity scale, and Gr the Grashof number defined as:

$$Gr=\frac{\beta g(T_H-T_C)H^3}{\nu^2}. \tag{6}$$

Thus, the dimensionless variables are the following:

$$\mathbf{u}^*=\left[\frac{Gr^{-1/2}H}{\nu}\right]\mathbf{u},\qquad \boldsymbol{x}^*=\left[\frac{1}{H}\right]\boldsymbol{x},\qquad t^*=\left[\frac{Gr^{1/2}\nu}{H^2}\right]t,$$

$$p^*=\left[\frac{Gr^{-1}H^2}{\rho\nu^2}\right]p,\qquad T^*=\frac{T-T_C}{T_H-T_C}, \tag{7}$$

where the variables with the asterisk * are dimensionless. For convenience we drop * so that the dimensionless equations become:

$$\frac{\partial u}{\partial x}+\frac{\partial v}{\partial y}=0, \tag{8}$$

$$\frac{\partial u}{\partial t}+u\frac{\partial u}{\partial x}+v\frac{\partial u}{\partial y}=-\frac{\partial p}{\partial x}+Gr^{-1/2}\nabla^2u+v\frac{|Ta|^{1/2}}{Gr^{1/2}}\mathrm{sign}(\omega), \tag{9}$$

$$\frac{\partial v}{\partial t}+u\frac{\partial v}{\partial x}+v\frac{\partial v}{\partial y}=-\frac{\partial p}{\partial y}+Gr^{-1/2}\nabla^2v+T-u\frac{|Ta|^{1/2}}{Gr^{1/2}}\mathrm{sign}(\omega), \tag{10}$$

$$\frac{\partial T}{\partial t}+u\frac{\partial T}{\partial x}+v\frac{\partial T}{\partial y}=\frac{1}{PrGr^{1/2}}\nabla^2T, \tag{11}$$

$$\nabla^2=\frac{\partial^2}{\partial^2x}+\frac{\partial^2}{\partial^2y}. \tag{12}$$

The parameters appearing in equations 9-11 are the Prandtl number,

$$\mathrm{Pr} = \frac{\nu}{\kappa}, \tag{13}$$

and the Taylor number,

$$\mathrm{Ta} = \frac{4\omega^2 \mathrm{H}^4}{\nu^2}\mathrm{sign}(\omega). \tag{14}$$

Equation 14 is a specialized definition for the Taylor number used in this study. As described in section 2 two different patterns of the Coriolis effect occur when the rotation direction of the centrifuge is changed. If Ta takes its normal definition by removing sign(ω) from equation 14 the Coriolis effect will be expressed unclearly. From equation 14, according to the definition of ω in the present coordinate system, ω is a positive and Ta>0 when the centrifuge rotates counter-clockwise; whereas Ta<0 when the centrifuge runs in a clockwise direction.

Generally, the kinetic and thermal boundary conditions for crystal growth are difficult to propose adequately. In this work we adopt those simplified boundary conditions considered by Crochet et al.[16]. On all the walls of the boat the no-slip condition is applied, except on the free-surface where a stress-free condition is used. The upper and lower boundaries are subjected to a linear temperature gradient. At both ends of the boat the temperature is held constant. Therefore, the boundary conditions in dimensionless form are:

$$x = 0, 0 \le y \le \mathrm{H}: \qquad \mathrm{u} = 0, \mathrm{v} = 0, \mathrm{T} = 1; \tag{15}$$

$$x = \mathrm{L}, 0 \le y \le \mathrm{H}: \qquad \mathrm{u} = 0, \mathrm{v} = 0, \mathrm{T} = 0; \tag{16}$$

$$0 \le x \le \mathrm{L}, y = 0: \qquad \mathrm{u} = 0, \mathrm{v} = 0, \mathrm{T} = 1 - x/\mathrm{L}; \tag{17}$$

$$0 \le x \le \mathrm{L}, y = \mathrm{H}: \qquad \frac{\partial \mathrm{u}}{\partial y} = 0, \mathrm{v} = 0, \mathrm{T} = 1 - x/\mathrm{L}. \tag{18}$$

NUMERICAL METHOD

The SIMPLE algorithm was employed for the simulation. We use the finite volume method with the pressure-velocity correction technique to solve the governing equations 8-11. The finite volume method divides the flow regimes into small control volumes, also called a staggered grid, illustrated in Figure 4. The pressure p and the temperature T are defined at the center, and the velocity components u, v on the faces of each control volume. The pressure-velocity correction, which is used to improve a guessed pressure distribution and to solve the velocity field, is derived via the continuity equation. A detailed description can be seen in reference[18].

In the process of formulating the discretization equations from the governing equations one problem encountered is how to discretize the convective and diffusive term exactly. Four proposed schemes are[18]: the central difference scheme, the upwind scheme, the hybrid scheme and the power-law scheme. The easy way to judge which scheme is best is to compare the computed results with those obtained by other numerical methods. For the present work we chose the central difference scheme. A comparison of these four schemes is presented in the next section.

The employed numerical method has the following characteristics: staggered control volumes, central-difference discretization for diffusive and advective fluxes, and fully implicit steady and time-marching schemes.

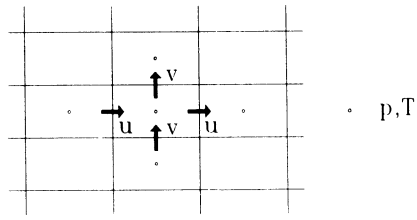

Figure 4. The staggered finite control volume and locations of variables u, v, p and T.

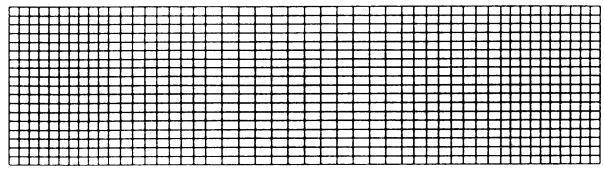

Figure 5. The 50×20 nonuniform mesh used in this study.

RESULTS AND DISCUSSION

In this section we consider the case of a constant Prandtl number, Pr=0.02, and an aspect ratio L/H=4. A 50×20 nonuniform mesh was designed to handle the high gradients near the vertical walls of the boat, as shown in Figure 5. The time-dependent convection is started from rest and the melting-point temperature is assumed everywhere at t=0. The time step for the time-marching scheme is 0.02.

The flow and temperature fields of the melt are displayed by using streamlines and isotherms. The stream function ψ is defined via the relations:

$$\frac{\partial \psi}{\partial y} = \mathrm{u}, \qquad \frac{\partial \psi}{\partial x} = -\mathrm{v}. \tag{19}$$

The time-dependent behavior of the melt can be found from the kinetic energy:

$$K = \frac{1}{2}\int_{\Omega}(\mathrm{u}^2 + \mathrm{v}^2)\mathrm{d}\Omega \tag{20}$$

where Ω is the melt flow domain.

First of all, we excluded the Coriolis force from the problem and studied only the effect of high gravity. Without the Coriolis effect (i.e. Ta=0) our model is much similar to those described in references[16,17]. Therefore, we can easily make a comparison between the algorithm of this study and the finite element method[16] or the Tau-Chebyshev pseudospectral method[17]. This comparison helped us to catch on more to the four schemes described in the above section. The results at Ta=0 computed by the four schemes are shown in Figure 6.

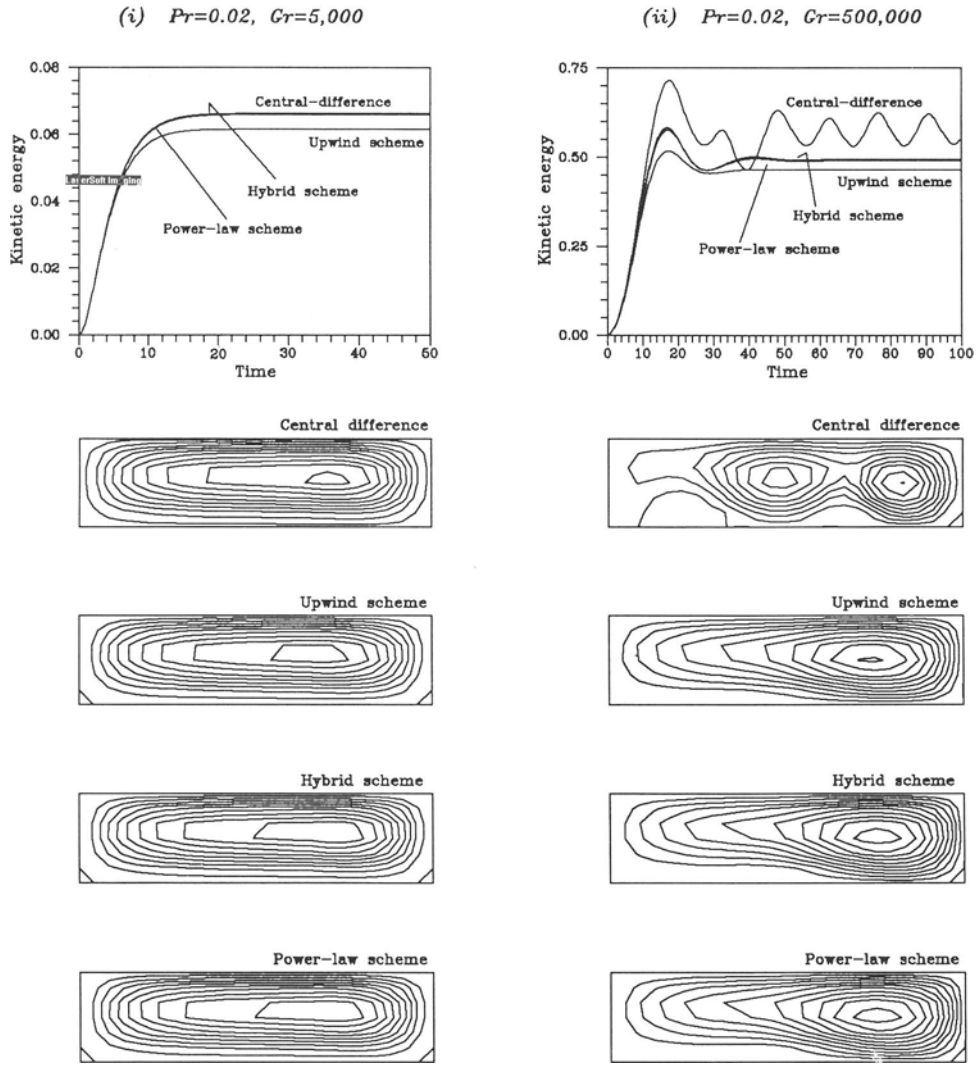

Figure 6. A comparison among four schemes: the central difference scheme, the upwind scheme, the hybrid scheme, and the power-law scheme. Gr=5×10^3 and 5×10^5 at Ta=0 and Pr=0.02. The streamlines are plotted at t=50(left) and t=100(right), respectively.

When the Grashof number is low ($Gr = 5 \times 10^3$) the kinetic energies and streamlines plotted in the left part are in a good agreement. But, when Gr is high enough, e.g. $Gr = 5 \times 10^5$, the schemes produce two different types of results. The central difference scheme gives an oscillatory solution whereas those obtained by the other three schemes are steady. The central difference scheme, compared with the finite element method[16] and the Tau-Chebyshev pseudospectral method[17], is valid for the time-dependent simulation of the present study. The difference among the results produced by the four schemes when Gr is high is a consequence of diffusive-type errors on the discretization.[19] The results for the different schemes should be the same if calculations are taken on a finer grid. Bottaro and Zebib[20] gave a detailed discussion on the problem of discretization and showed that a designed coarser grid, when the central difference scheme is used, provides the solutions agreeing well with those obtained by a very fine grid.

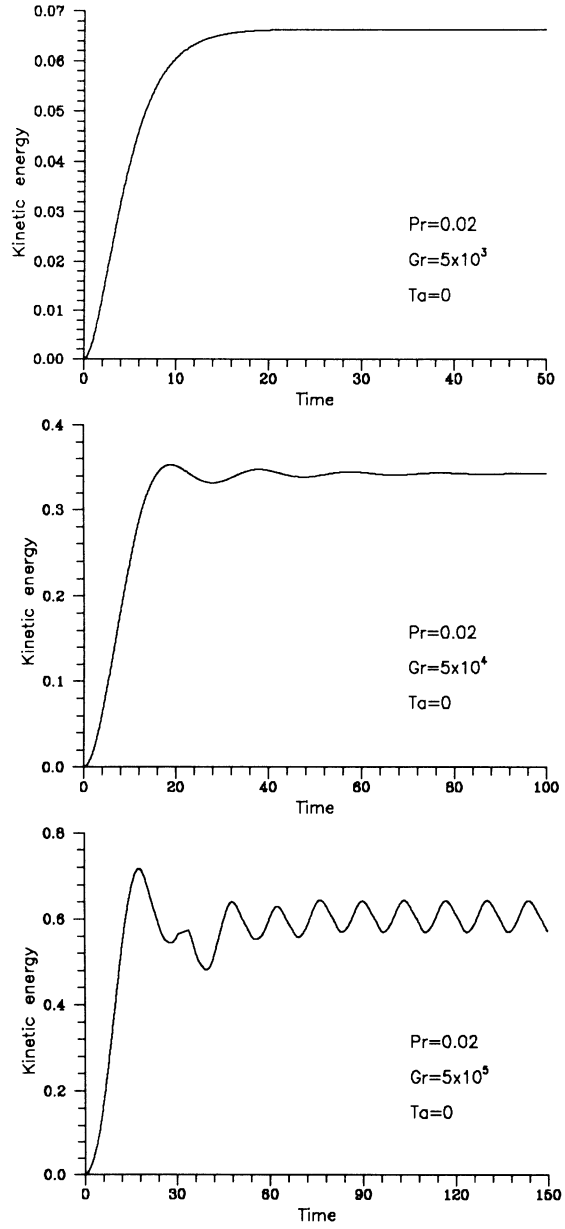

Figure 7. The time evolution of the kinetic energy K for Gr= (a)5×10^3, (b)5×10^4, and (c)5×10^5 at Ta=0 with Pr=0.02.

The unsteady behavior of melt flow at Ta=0 is illustrated by the time evolution of the kinetic energy K. Figure 7 presents them for three Gr, 5×10^3, 5×10^4 and 5×10^5. In the case of $Gr=5\times10^3$, K approaches a steady value. From Figure 6 we see only one convective roll in the boat. When Gr reaches 5×10^4, a moderate value, K implies a dampened oscillatory solution. If Gr increases high enough, e.g. at 5×10^5, K no longer converges but is periodic after several cycles. The flow at $Gr=5\times10^5$ is oscillatory. We plot the streamlines and isotherms at several typical times in Figure 8. At first the melt rises at the hot wall, moves from left to right, and descends at the cold wall. After that the flow structure becomes quite complex. The primary convective roll is not a single one but presents patterns of two or three co-rotating vortices. Meanwhile, some small eddies are generated at the bottom of the boat. During one period of oscillation the primary convective

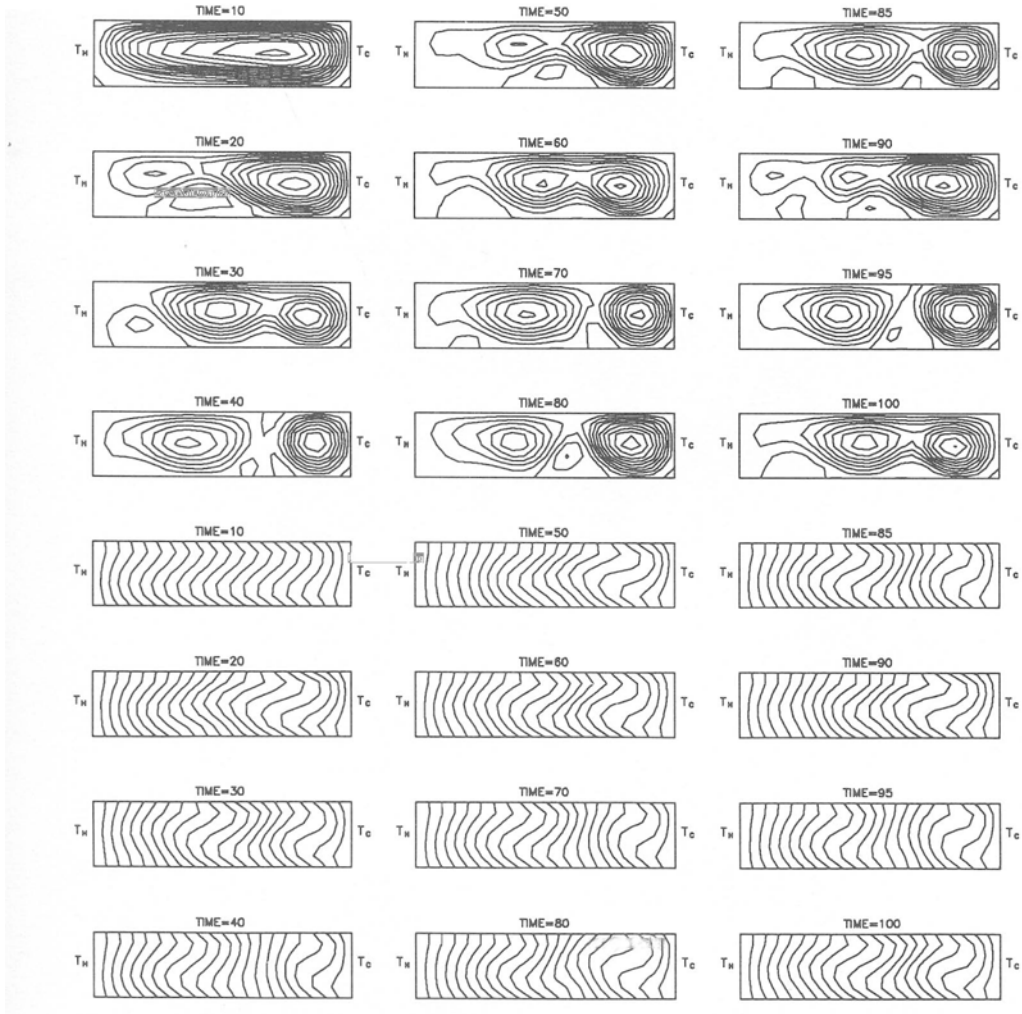

Figure 8. Streamlines and isothermal at several times for $Gr=5\times10^5$, Ta=0 and Pr=0.02.

roll is divided or merged accompanied by the growth or decay of these small eddies.

The melt flow at Ta=0 can be considered gravity-dependent via Gr, when the temperature difference between the ends of the boat is held constant. From the above results we see that centrifugal acceleration may enhance the strength of convection and induce oscillation in the melt but does not make stabilize the melt flow.

In the following, we take the Coriolis force into account. To evaluate the Coriolis effect on the melt flow, especially on oscillatory convection, the case at $Gr = 5\times10^5$ is considered. The simulations were performed for a variety of |Ta|, from 1×10^4 to 1×10^9. When |Ta| is less than 1×10^8, no difference between these results and those at Ta=0 can be observed. However, when |Ta| reaches 1×10^9 the results shown in Figure 9 are much more interesting. Figure 9(a) shows the time evolution of the kinetic energy K for $Gr = 5\times10^5$ and $Ta = 1\times10^9$. According to the definition 14 the centrifuge rotates counterclockwise if $Ta = 1\times10^9$. Comparing with Figure 7(c), the melt flow still maintains a sustained periodic oscillation. The strength of the convection seems to be enhanced by the Coriolis force. When the centrifuge runs in clockwise direction, i.e. $Ta = -1\times10^9$, the result shown in

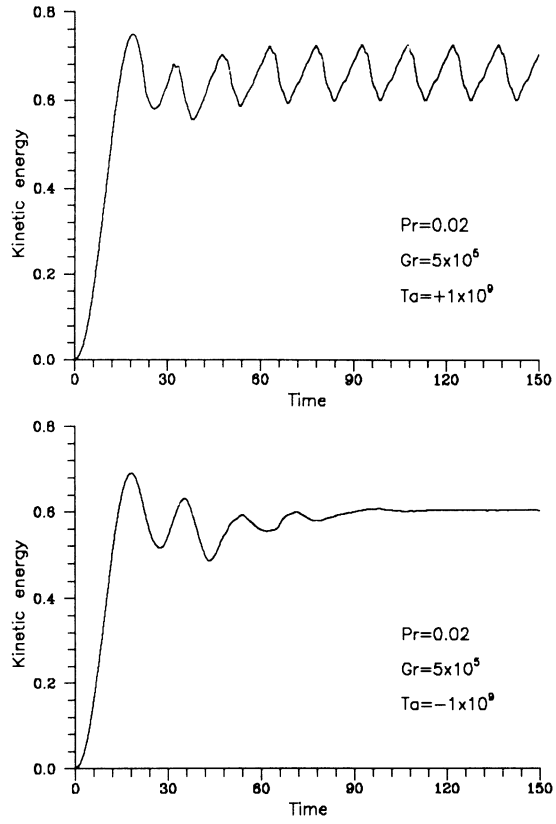

Figure 9. The time evolution of the kinetic energy K for $Gr=5\times10^5$, Ta= (a)1×10^9 and (b)-1×10^9, and Pr=0.02.

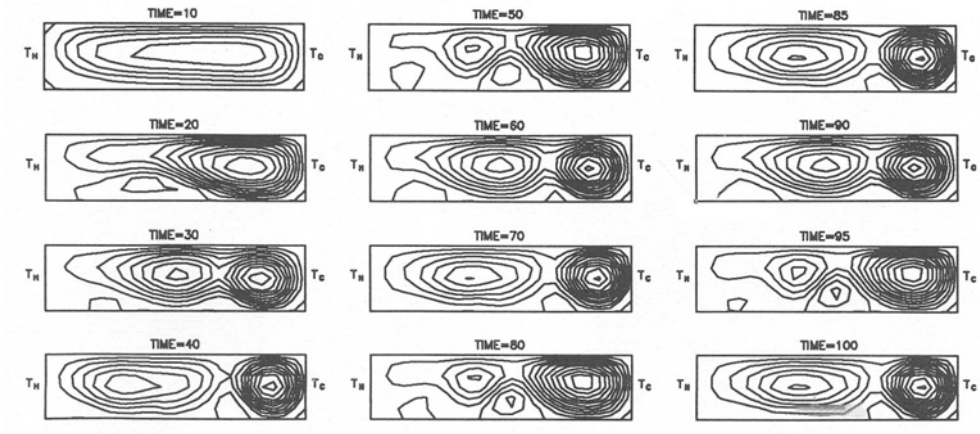

Figure 10. Streamlines at several times for $Gr=5\times10^5$, $Ta=1\times10^9$ and Pr=0.02.

Figure 9(b) approaches a steady value, and the melt flow is not oscillatory, but steady.

The results lead to a reexamination of stabilizing effects due to the Coriolis force observed in our model experiments[15]. It must be noted that the Coriolis force does not affect the melt flow by doing work. It influences the melt flow by altering the flow pattern, and then the balance of the system energy. In order to analyze the Coriolis effect on the flow

structure, we plot the streamlines in Figure 10 for $Ta = 1 \times 10^9$ at several typical times and in Figure 11 for $Ta = -1 \times 10^9$ at one time when the flow becomes steady. The isotherms for these two cases are nearly the same as those at Ta=0 and not presented here. The calculations demonstrate that the Coriolis effect on the melt is not so easy as shown in Figure 3. Both cases (I and II) may coexist in the flow regimes. Analysis reveals that, for $Ta = 1 \times 10^9$, the primary convective rolls tend to be cut by the Coriolis force when it helps the small eddies to grow. This indicates that the flow could not become steady but more oscillatory. On the contrary, the effects of the Coriolis force are opposite completely if $Ta = -1 \times 10^9$. This time the Coriolis force expands the primary vortex but prevents the growth of the small eddies. This is perhaps the reason why the steady state of the melt does occur.

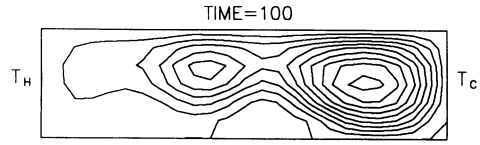

Figure 11. Streamlines for $Gr=5 \times 10^5$, $Ta=-1 \times 10^9$ and Pr=0.02 at t=100, at which the melt flow has become steady.

CONCLUSIONS

A numerical investigation was carried out for melt flow in a simplified two-dimensional rectangular boat influenced by both high gravity (i.e. the centrifugal acceleration) and the Coriolis force. The results show that the Coriolis force may have a stabilizing influence on melt flow but only under the conditions of co-rotation of the centrifuge and the main fluid flow of the melt within a certain range of Taylor number. When the Coriolis force is not involved the same stabilizing effect of high gravity does not occur. The results in this numerical study verify the observation of model experiments[15], and partially explain why the striations of the grown GaAs crystals become weak or fade away..

In the present study we assume fixed temperature boundary conditions. The isotherms move only slightly for all the simulations. However, in all actual processes of crystal growth heat is exchanged between the melt and its growth environment, and the temperature field varies significantly. Thus a further study of the influence of large centrifugal acceleration and the Coriolis force on crystal growth, espeacially in considering radiative heat transfer on the surface of the melt and a solid-liquid interface, is needed. Moreover, a three-dimensional calculation also must be considered indispensable.

ACKNOWLEDGMENTS

The present work was initially partly supported by the National Natural Sciences Foundation of China and subsequently by the Chinese Academy of Sciences. The simulations was performed on Alliant FX/40 computer of the institute of Mechanics. The two first authors wish to acknowledge youth research scholarships from the Institute of Mechanics. Also we would like to thank Professor G. Müller and Mr. J. Friedrich of Universität Erlangen-Nürnberg for their valuable comments and suggestions concerning this paper.

REFERENCES

1. J.R. Carruthers, *J. Crystal Growth* 32:13 (1976).
2. W.E. Langlois, *Ann. Rev. Fluid Mech.* 17:191 (1985).
3. G. Müller, "Crystal Growth from the Melt," Springer, Berlin (1988).
4. G. Müller, P. Kyr and E. Schmidt, *J. Crystal Growth* 49:387 (1980).
5. G. Müller, G. Neumann, *J. Crystal Growth* 59:548 (1982).
6. G. Müller, G. Neumann, *J. Crystal Growth* 63:58 (1983).
7. G. Müller, *J. Crystal Growth* 99:1242 (1990).
8. W. Weber, G. Neumann and G. Müller, *J. Crystal Growth* 100:145 (1990).
9. G. Müller, G. Neumann and W. Weber, *J. Crystal Growth* 119:8 (1992).
10. H. Rodot and L.L. Regel, *J. Crystal Growth* 79:77 (1986).
11. H. Rodot and L.L. Regel, *J. Crystal Growth* 104:280 (1990).
12. X.R. Zhong, B.J. Zhou, Q.M. Yan, F.N. Cao, C.J. Li, L.Y. Lin and W.J. Ma, Y. Zheng, F. Tao, M.L. Xue, *J. Crystal Growth* 119:74 (1992).
13. B.J. Zhou, F.N. Cao, L.Y. Lin and W.J. Ma, Y. Zheng, F. Tao, M.L. Xue, Growth of GaAs single crystals under high gravity conditions, "The 2nd International Workshop Materials Processing in High Gravity," Potsdam, New York, (June 1993).
14. W.A. Arnold, W.R. Wilcox, F. Carlson, A. Chait and L.L. Regel, *J. Crystal Growth* 119:24 (1992).
15. W.J. Ma, F. Tao, Y. Zheng, M.L. Xue and B.J. Zhou, L.Y. Lin, Response of temperature oscillations in a Tin melt to the effects of centrifuge, "The 2nd International Workshop Materials Processing in High Gravity," Potsdam, New York, (June 1993).
16. M.J. Crochet, F.T. Geyling and J.J. Van Schaftingen, Finite element method for calculating the horizontal Bridgman growth of semiconductor crystals, in: "Finite Elements in Fluids-Volume 6," R.H. Gallagher, G.F. Garey, J.T. Oden and O.C. Zienkiewicz, ed., John Wiley & Sons, Chichester (1985).
17. J.P. Fontaine, E. Crespo del Arco, A. Randriamampianina, G.P. Extrémet and P. Bontoux, *Adv. Space Res.* 8:265 (1988).
18. S.V. Patankar. "Numerical Heat Transfer and Fluid Flow," Hemisphere, Washington, D.C. (1980).
19. W.J. Minkowycz, E.M. Sparrow, G.E. Schneider and R.H. Pletcher, "Handbook of Numerical Heat Transfer," John Wiley & Sons, New York (1988).
20. A. Bottaro and A. Zebib, *Phys. Fluids*, 31:495 (1988).